Proceedings World Geothermal Congress 2015
Melbourne, Australia, 19-25 April 2015

Thermodynamic Analysis of Double-Stage Organic Rankine Cycles for Low-Enthalpy Sources Based on a Case Study for 5.5 MWe Power Plant Kirchstockach (Germany)

Florian Heberle*, Thomas Jahrfeld[+] and Dieter Brüggemann*

*Lehrstuhl für Techn. Thermodynamik und Transportprozesse, Universität Bayreuth, Universitätstr. 30, 95447 Bayreuth, Germany

[+]renerco plan consult GmbH, Herzog-Heinrich-Strasse 13, 80336 München, Germany

florian.heberle@uni-bayreuth.de, thomas.jahrfeld@renerco.com, brueggemann@uni-bayreuth.de

Keywords: Geothermal Power Generation, Organic Rankine Cycle, Double-Stage Process, Kirchstockach

ABSTRACT

Geothermal power generation by organic Rankine cycle (ORC) is examined in a case study for the 5.5 MWe double-stage power plant in Kirchstockach, Germany. The power plant consists of two structurally similar modules operating at high (HT) and low pressure (LT) level. In both units R245fa is chosen as working fluid. A simulation model is validated based on operational data of the power plant and shows a good agreement. The calculations are performed using the fluid property databases RefProp and StanMix. A significant deviation of about 10 % between the databases is observed for the enthalpy difference at expansion due to deviation in the prediction of the slope of the saturation curve. Considering operational data and actual estimations in literature the isentropic efficiency of the turbine calculated by StanMix seems to be more reliable. Furthermore, sensitivity analyses and comparisons to alternative power plant concepts are performed based on the validated model. A variation of the split ratio of the geothermal fluid at the outlet of the LT-evaporator shows a maximum of the second law efficiency for a ratio of 3:1 (HT:LT). A comparison of the double-stage concepts to single-stage ORC using pure fluids and zeotropic mixtures shows the highest gross second law efficiency for the single-stage concept and R134a/R245fa as working fluid. However, ORC units using R134a, R600a or these fluids as mixture component lead to high power requirement regarding the feed pump. As result the investigated double-stage concept lead to the highest net efficiencies of the considered optimization strategies.

1. INTRODUCTION

Studies on the potential of geothermal energy generation show a significant potential for low-temperature resources (Bertani, 2003; Stefansson, 2000). Therefore binary power plants, like the Organic Rankine Cycle (ORC) or Kalina Cycle, are suitable as power generation units. In these systems the thermal energy of the geothermal fluid is coupled to a secondary thermodynamic cycle, where a low-boiling working fluid is evaporated at a moderate pressure level. The generated vapor flow is expanded in a turbine-generator unit to a lower pressure level. The cycle is closed by condensing the working fluid and forcing the liquid phase to a higher pressure level by a feed pump. Single-stage ORC systems consisting of one preheater, evaporator, turbine and condenser, are state-of-the-art technologies. The first geothermal ORC power plant was set in operation in Russia in 1967 (Lund, 2004). The standard concept can be adapted to different temperatures of the geothermal fluid by selecting an appropriate working fluid. For the typical temperature range of the heat source between 80 °C and 200 °C, refrigerants and natural hydrocarbons are favorable. In general, the geothermal power generation by ORC is limited by the minimal temperature difference, so called pinch point, between the heat source or sink and the ORC. Innovative concepts to reduce this limitation and to increase the cycle efficiency are the transcritical cycle, the pinch-point smoothing, the use of zeotropic mixtures or the double-stage ORC concepts.

In this paper the double-stage concept is analyzed under thermodynamic criteria. Two ORC modules operating at different pressure levels enable a better match of the power generation unit to the temperature profile of the geothermal resource compared to the single-stage concept. In this context a reduction of exergy losses can be observed. Based on the realized double-stage ORC power plant in Kirchstockach (Germany) with an electrical power of 5.5 MW (installed electric capacity of the generator 7.0 MW) and R245fa (1,1,1,3,3-pentafluoropropan) as working fluid, a simulation model is validated by operational data. In this context two potential fluid property databases and their reliability are compared. Sensitivity analyses are performed concerning the split ratio of the geothermal fluid mass flow rate and ORC working fluid selection. Furthermore, a thermodynamic comparison of alternative ORC concepts, in particular the single-stage system and the use of zeotropic mixtures, is presented.

2. DOUBLE-STAGE ORC IN KIRCHSTOCKACH, GERMANY

In literature the terms double-stage, two-stage or two-level ORC is associated with different power plant concepts. Kosmadakis et al. (2010a and 2010b) and Preißinger et al. (2012) describe a cascading system as double-stage ORC for solar and biomass applications. In these studies the evaporation of a lower boiling working fluid is realized by the condensation of a higher boiling working fluid. In addition, ORC systems which include two expanders in series are labeled as two-stage ORC (Smolen, 2011). Meinel et al. (2014) extend such a two-stage expansion by a saturator to use extracted vapour from the first stage turbine for internal heat recovery. In two-level or two-pressure systems examined by Drescher (2008) and Walraven et al. (2013) the ORC mass flow is splitted at the outlet of the low-temperature preheater into a low and high pressure stream. At outlet of the turbines both streams are mixed again and the condensation as well as the pressure rise to the lower level take place in one component each. For a better modularization also separate ORC systems are suitable for a two-stage concept. Therefore, two identically structured modules could be arranged in series. The module supplied with the higher temperature of the geothermal fluid operates at higher ORC pressures. A further development of this concept in form of splitting the geothermal mass flow is examined by Kanoglu (2002). The double-stage ORC in Kirchstockach (Germany) analyzed in this work is shown in Figure 1. The power plant consists of two separate ORC modules a high-temperature (HT) and a low-temperature (LT) ORC. The power plant has been in operation

since 2013 and has a nominal electric capacity of 5.5 MW referred to an ambient temperature of 8 °C, a mass flow rate of 120 kg/s and a temperature of 138 °C of the geothermal fluid.

Figure 1: Double-stage ORC power plant in Kirchstockach, Germany (Source: Geothermie Kirchstockach)

A scheme of the power plant is shown in Figure 2. In both ORC modules, the same working fluid (R245fa) is used due to advantages with respect to storage and legal requirements. The two modules are nearly identically structured. The HT-ORC operates at higher pressure compared to the LT-ORC. The thermal energy of the geothermal fluid is coupled to the ORC in the preheater and the evaporator of each module. In case of the HT-ORC the preheating is divided into two steps, the LHT- and HHT-preheater. Therefore the mass flow of the geothermal fluid is separated at the outlet of the LT-evaporator and coupled parallelly to the LT- and HT-cycle. In general, at the outlet of the evaporators saturated vapour is obtained and expanded in the turbine. Furthermore, an air-cooled condenser and a feed pump are part of each module.

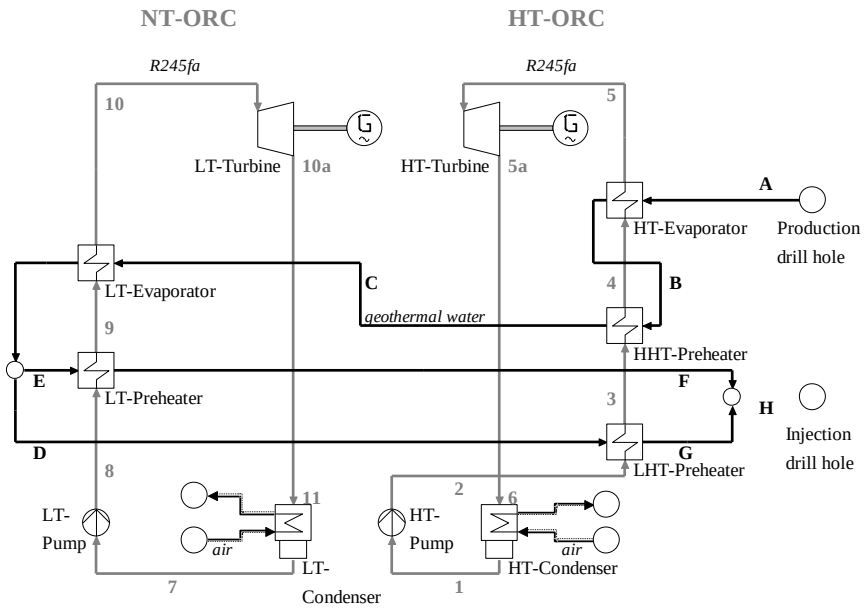

Figure 2: Scheme of the double-stage ORC power plant in Kirchstockach, Germany

3. METHODOLOGY

3.1 Process simulations

The steady-state process simulations are performed using the software Cycle Tempo V5.0 (Woudstra and van der Stelt, 2002). The calculation of fluid properties is based on the databases RefProp V9.1 (Lemmon et al., 2013) and StanMix (Angelino and Colonna di Paliano, 1998). Within RefProp the model of Lemmon and Span (2006) is used for R245fa. All properties of fluid mixtures in this work are calculated by RefProp and the model of Kunz et al. (2007). For the simulations heat losses are neglected. Operational data from the real power plant serve for input data regarding the simulation and validation of the results. The data are collected at full load and the ambient temperature corresponds to the design point of the power plant (T_{amb} = 8 °C). Boundary conditions for the

simulation are set as constant, like mass flow rate and temperature of geothermal fluid or pressure levels of the ORC modules are highlighted in Table 3.

3.2 Turbine efficiency

Operational data of the temperature at the outlet of the LT- and HT-turbine are not available due to missing measurement devices. Therefore, the isentropic efficiency $\eta_{s,T}$ is calculated based on Equation (1) and manufacturer design data for pressure p and temperature T at turbine inlet and outlet. The design parameters T_{in}^{Design}, p_{in}^{Design}, T_{out}^{Design} and p_{out}^{Design} are listed in Table 1. The manufacturer indicates the tolerance of the design parameters with ± 1 °C for temperatures and ± 0.2 °bar for pressures.

$$\eta_{s,T} = \frac{h_{in} - h_{out}}{h_{in} - h_{s,out}} \tag{1}$$

The enthalpy at inlet h_{in} and outlet h_{out} is calculated by RefProp and StanMix based on the temperature and pressure at inlet and outlet of the turbines at the design point. $h_{s,out}$ represents the enthalpy in case of isentropic expansion. In Table 1, the resulting isentropic efficiencies of the turbines are listed.

Table 1: Isentropic efficiency of the LT- and HT-turbine based on design data

Turbine	T_{in}^{Design} (°C)	T_{out}^{Design} (°C)	p_{in}^{Design} (bar)	p_{out}^{Design} (bar)	$\eta_{s,T}^{RefProp}$ (%)	$\eta_{s,T}^{StanMix}$ (%)
HT	106.7	48.5	13.3	1.3	81.78	88.28
LT	72.5	38.8	5.8	1.2	75.26	82.72

Obviously the chosen databases for fluid properties lead to a significant difference in the calculated isentropic efficiencies of the turbines, which are considerably lower using RefProp fluid properties. The described difference would lead to noticeable deviations regarding the simulations and estimation of power output as well as cycle efficiency. To analyse the reliability of the fluid properties calculated by RefProp and StanMix a comparison to alternative equation of states (EOS) and experimental data is discussed briefly in the next paragraph.

In Table 2 the enthalpy difference at expansion dh_T is shown for RefProp and StanMix as well as for the Peng-Robinson EOS (Peng and Robinson, 1976) and Redlich-Kwong Soave EOS (Soave, 1972).

Table 2: Enthalpy difference at expansion for selected EOS

Turbine	$dh_T^{RefProp}$ (kJ/kg)	$dh_T^{StanMix}$ (kJ/kg)	dh_T^{PR} (kJ/kg)	dh_T^{RKS} (kJ/kg)
HT	35.90	39.21	39.43	39.72
LT	21.85	24.37	24.47	24.56

The results show that the enthalpy differences calculated by StanMix are in a good agreement with Peng-Robinson EOS and Redlich-Kwong Soave EOS. The relative deviations between these models range between 0.13 % and 1.30 %. In contrast, the values calculated by RefProp show differences up to 10.34 % compared to StanMix. Extensive analysis of the fluid properties and comparison to experimental data shows that the heat capacity of the liquid phase shows high deviations for RefProp and StanMix. In Figure 3 the heat capacity for the liquid phase of R245fa depending on temperature is shown. In addition, experimental data of Hwang et al. (Hwang et al., 1992) are included. The deviation of the liquid heat capacity, calculated by RefProp and StanMix, increase with rising temperature. Near the critical temperature the use of RefProp lead to 32.36 % lower values compared to StanMix. In context of relevant process parameters for the examined double-stage ORC, the liquid heat capacity calculated by StanMix is 2.72 % lower (condensation level) respectively 6.76 % higher (HT-evaporation level) compared to RefProp. The slope of the dew line in the *T*,*s*-diagram differs noticeably between the considered EOS due to the structure of the EOS and the considered heat capacity of the ideal gas. The normalized *T*,*s*-diagram ($s(T = 20\ °C;\ x = 0) = 1$) of Figure 4 illustrates in particular the deviations for fluid properties in case of saturated or slightly superheated states, which leads to the differences of dh_T listed in Table 2. The differences are considerably weakened in case of relevant superheating. Exemplarily, a superheating of 10 K decreases the deviation of $dh_{T,HT}$ to 3.83 % between RefProp and StanMix. The same interrelation between deviations of heat capacity and deviations of enthalpy differences at expansion can be observed for R134a. In case of natural hydrocarbons like isobutane (R600a) or isopentane (R601a) the deviations are less pronounced. A comparison of RefProp and StanMix to experimental data for the liquid density of R245fa shows good agreement. The averaged deviation in case of RefProp is 0.07 % and for StanMix 1.96 %. A validation or clear statement concerning the reliability of the examined EOS is not possible due to the lack of experimental data in the gas phase. Nevertheless, the isentropic efficiencies of the turbine based on StanMix seem to be more reliable and are used in the simulations. In this context, a comparison to real power plant data available in literature shows that the values calculated by RefProp are reached and partly exceeded by small scale units and power plants set in operation in 1989 and 2001 (Aneke et al., 2011; Kanoglu, 2002; Bayerisches Landesamt für Umweltschutz, 2001). Actual theoretical studies regarding geothermal power generation assume 85 % for isentropic efficiency of the turbine (Astolfi et al., 2014).

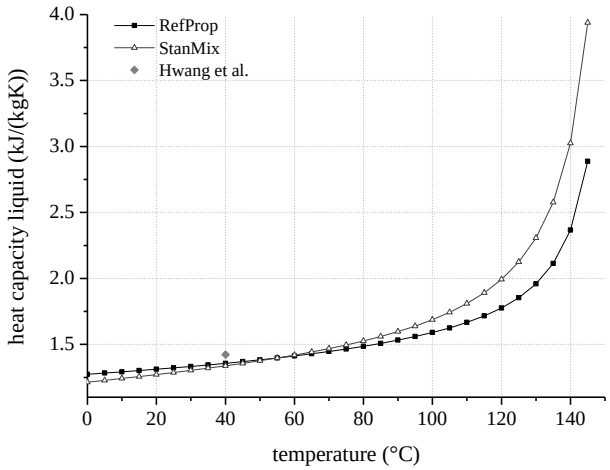

Figure 3: Liquid heat capacity of R245fa depending on temperature

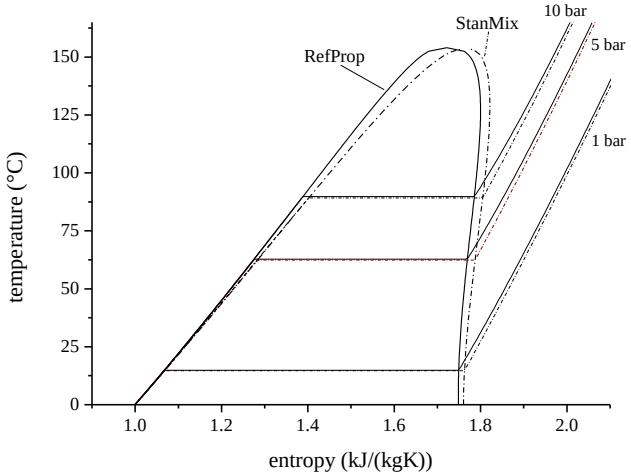

Figure 4: Normalized *T,s*-diagram of R245fa based on the databases RefProp and StanMix

3.3 Analysis

The simulation results are analyzed according to the second law of thermodynamics. Therefore, gross and net second law efficiencies of the ORC system are calculated based on the power output of the turbine P_T and the power consumption of the feed pump P_P. Other parasitic power requirements regarding the well pump or fans for the air condenser are not considered.

$$\eta_{II,gross}^{ORC} = \frac{P_T}{\dot{E}_{GF}} \tag{2}$$

$$\eta_{II,net}^{ORC} = \frac{P_T - P_P}{\dot{E}_{GF}} \tag{3}$$

The maximum power output of the geothermal source, the exergy flow $\dot{E}_{GW}$, is obtained by multiplying the specific exergy with the mass flow rate of geothermal fluid $\dot{m}_{GF}$:

$$\dot{E}_{GF} = \dot{m}_{GF} e \tag{4}$$

The specific exergy e is based on:

$$e = h - h_0 - T_0(s - s_0) . \tag{5}$$

The state variables temperature T_0, enthalpy h_0 and entropy s_0 are related to ambient conditions. Regarding the validation of the simulation model, the relative deviation of the real power plant data and the simulation results is calculated by

$$rd = \frac{|\Delta X| \cdot 100\%}{X} . \tag{6}$$

4. RESULTS

4.1 Validation

The simulation using the fluid property databases RefProp and StanMix are validated based on real power plant data shown in Table 2. Additionally, the relative deviation between the power plant data and the simulation results is listed.

Table 3: Real power plant data, simulation results and the corresponding relative devaitions

No.	Parameter	Real power plant data	Simulation RefProp	Simulation StanMix	*rd* / % RefProp	*rd* / % StanMix
HT-ORC						
1	Pump inlet temperature (°C)	22.71	23.04	22.81	0.11	0.03
1	Pump inlet pressure (bar)*	1.49	1.49	1.49	0.00	0.00
1	Mass flow rate (kg/s)	99.66	111.01	109.61	11.39	9.98
2	Pump outlet temperature (°C)	n.a.	24.22	24.01	–	–
2	Pump outlet pressure (bar)*	15.24	15.24	15.24	0.00	0.00
3	Preheater (HHT) inlet temperature (°C)	62.23	59.47	60.23	0.82	0.60
4	Preheater (HHT) outlet temperature (°C)	99.40	103.08	103.16	0.99	1.01
5	Evaporator outlet temperature (°C)	103.79	104.15	104.23	0.10	0.12
5	Evaporator outlet pressure (bar)*	13.85	13.85	13.85	0.00	0.00
5a	Turbine outlet temperature (°C)	n.a.	44.09	47.7	–	–
LT-ORC						
7	Pump inlet temperature (°C)	22.88	23.24	23.03	0.12	0.05
7	Pump inlet pressure (bar)*	1.55	1.55	1.55	0.00	0.00
7	Mass flow rate (kg/s)	57.80	70.72	69.72	22.35	20.61
8	Pump outlet temperature (°C)	n.a.	23.71	23.51	–	–
8	Pump outlet pressure (bar)*	6.75	6.75	6.75	0.00	0.00
9	Preheater outlet temperature (°C)	61.56	67.22	67.37	1.69	1.74
10	Evaporator outlet temperature (°C)	68.72	69.22	69.37	0.15	0.19
10	Evaporator outlet pressure (bar)*	5.97	5.97	5.97	0.00	0.00
10a	Turbine outlet temperature (°C)	n.a.	37.46	40.02	–	–
Geothermal fluid						
A	HT evaporator inlet temperature (°C)*	135.14	135.14	135.14	0.00	0.00
A	Total mass flow rate (kg/s)*	122.37	122.37	122.37	0.00	0.00
B	HHT preheater inlet temperature (°C)	105.47	106.94	106.96	0.39	0.39
C	LT evaporator inlet temperature (°C)*	92.95	92.95	92.95	0.00	0.00
D	LHT preheater inlet temperature (°C)*	70.37	70.37	70.37	0.00	0.00
D	LHT mass flow rate (kg/s)*	67.89	67.89	67.89	0.00	0.00
E	LT preheater inlet temperature (°C)*	70.37	70.37	70.37	0.00	0.00
E	LT mass flow rate (kg/s)*	54.48	54.48	54.48	0.00	0.00
F	LT preheater outlet temperature (°C)	51.62	51.84	52.13	0.07	0.16
G	LHT preheater outlet temperature (°C)	51.66	51.66	51.66	0.00	0.00
H	Injection temperature (°C)	51.50	51.87	51.87	0.11	0.11
	ORC gross generator power (kW)	5313.41	5288.85	5309.64	0.46	0.07
	LT feed pump (kW)	60.67	59.76	59.76	1,52	1.52
	HT feed pump (kW)	234.15	225.96	226.21	3.62	3.51
	ORC gross second law efficiency (%)	52.26	52.01	52.22	0,46	0.07
	ORC net second law efficiency (%)	49.36	49.20	49.41	0.31	0.01
	Ambient temperature (°C)	8.67	8.67	8.67	0.00	0.00

*set variables for simulation

In general, the simulation results are in a good agreement to the real power plant data. Therefore, the simulation model can be used for further analysis. In average the relative deviation for the simulation based on RefProp and StanMix differs only slightly (0.48%). However, a significant difference for the outlet temperature of the turbines can be observed due to the behavior discussed in chapter 3.2. In this context, RefProp leads to 0.82 % (LT) and 1.14 % (HT) lower temperatures at the turbine outlet.

A calculation of the double-stage ORC based on RefProp and the turbine efficiency of Table 1 would lead to a power output of 4875 kW, 9 % below the measured value. Furthermore, the outlet temperature of the preheaters shows a noticeable deviation to the operational data. According to the design point of the power plant the preheater outlet temperature is set 2 K below the saturation temperature. In contrast, the real power plant data show a far higher subcooling at the evaporator inlet. Finally, the LT- and HT-ORC mass flow rate differs considerably from the operational data. According to the manufacturer, the uncertainties of the integrated flow rate sensors are responsible for this deviation. It should be highlighted here that the calculations of turbine efficiency in chapter 3.2 (see Equation 1) are independent of ORC mass flow rate. Regarding the reliability of the mass flow rate of the geothermal fluid, the measured value of Table 1 is compared to an additional implemented mass flow meter and doubled-checked by an external measurement device. In relation to the sensor used for the analysis, the alternative devices show a deviation below 1.69 %. This good agreement confirms the reliability of the cycle analysis and in particular the calculations of turbine efficiency.

4.2 Performance analysis

The second law efficiency of the examined double-stage power plant is higher compared to existing units with similar boundary conditions (DiPippo, 2005, 1999). The gross efficiency according to the first law thermodynamics is 12.29 % and the net efficiency is 11.62 %. The calculated isentropic efficiency of the LT-feed pump is 50 % and in case of the HT-feed pump 52 %. The temperature, enthalpy flow-diagram of Figure 5 illustrates the transmitted heat flow and a good match of the temperature profiles of heat source and ORC.

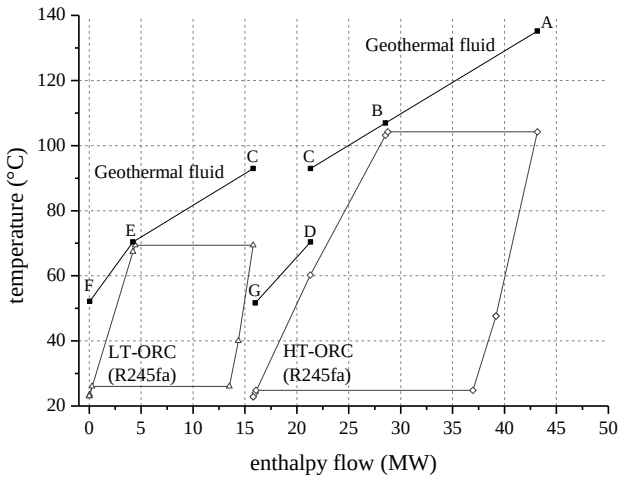

Figure 5: Temperature, enthalpy flow-diagram for the double-stage ORC in Kirchstockach

4.2 Sensitivity analysis

To identify the most efficient process parameters of the double-stage concept a variation of the LHT-mass flow rate (state points E and F) is performed. As boundary conditions, the geothermal parameters, turbine efficiencies, ORC pressures and pinch points of the heat exchangers (HT preheater, HHT preheater and LT preheater) are set constant. For the LHT-preheater a minimal pinch point of 3 K is defined. Figure 6 shows the gross second law efficiency and the temperatures of the geothermal fluid at the state points C and F as well as the LT-ORC mass flow rate as a function of the LHT mass flow rate of the geothermal fluid.

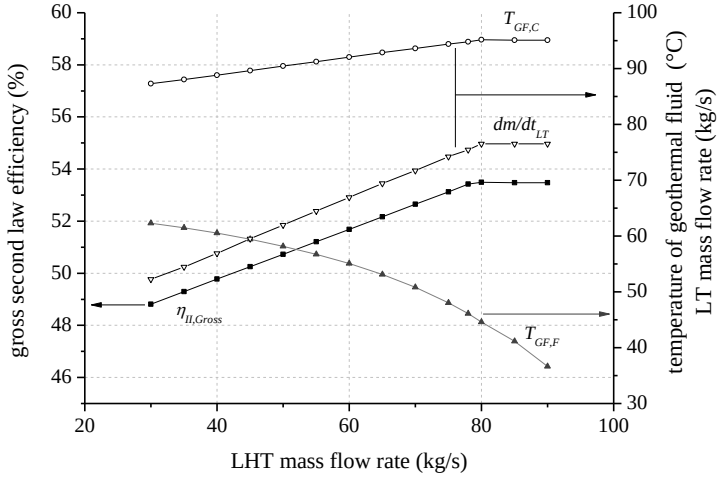

Figure 6: Gross second law efficiency and temperatures of the geothermal fluid at state points C and H as a function of the LHT mass flow rate

In the range of 30 kg/s and 80 kg/s the second law efficiency increases linearly with rising LHT mass flow rate. Due to an increasing LHT mass flow rate the LHT-preheater plays a bigger role in preheating the working fluid in the HT-ORC. In this context, the temperature of the geothermal fluid $T_{GF,C}$ in state point C increases considering the assumption of a constant pressure level in the HT-ORC and a constant pinch point in the HT-evaporator. As a result, the mass flow rate of the LT-ORC increases and the temperature of the geothermal fluid $T_{GF,F}$ in state point F decreases. Summing up, a higher thermal energy is coupled to the LT-ORC and the power output, respectively, the second law efficiency increases. The maximum efficiency is reached for 80 kg/s with 53.49 %. In case of a LHT mass flow rate higher than 80 kg/s the minimal pinch point in the LHT-preheater (3 K) is reached. Thus the temperature of the geothermal fluid $T_{GF,C}$ in state point C is constant at 95.1 °C. As a result, the mass flow rate of the LT-ORC and second law efficiency stay constant, too.

4.3 Alternative working fluids and concepts

In this chapter, a comparison of the examined double-stage power plant compared to alternative working fluids and configurations is presented. First the second law efficiency for selected working fluid combinations regarding the LT- and HT-ORC are calculated. In addition, the double-stage concept is compared to single-stage cycle with pure fluids and fluid mixtures.

4.3.1 Working fluids

Next to R245fa as a working fluid, common candidates like R600a and R134a are investigated. The low boiling refrigerant R134a seems to be suitable for the LT-module. Therefore, a combination of R134a (LT) and R245fa (HT) as well as R134a (LT) and R600a (HT) is considered. Furthermore a use of R600a in the LT and HT is investigated. For different working fluids in the LT- and HT-unit, an additional storage tank has to be installed. In the context of flammable fluids like R600a legal regulations and higher requirements regarding insurances have to be taken into account. For the simulations the boundary conditions like geothermal parameters, turbine efficiencies, pinch points of the heat exchangers and pressure losses are equal to the R245fa/R245fa system. The ORC pressure is maximal 80 % of the critical pressure.

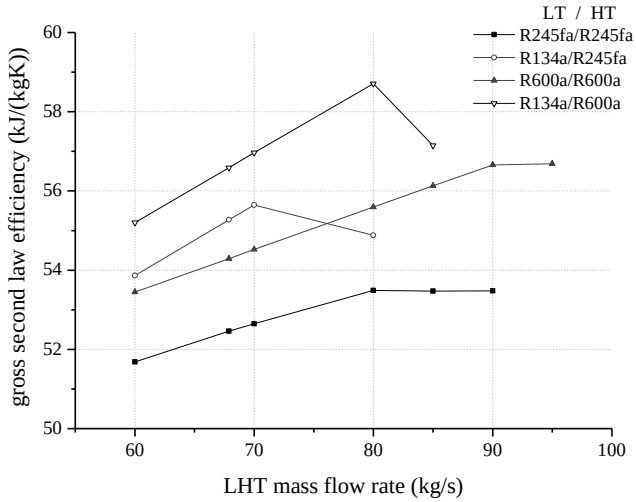

Figure 7: Gross second law efficiency depending on LHT mass flow rate

As indicated for R245fa/R245fa as well as for R600a/R600a the gross second law efficiency increases with increasing LHT mass flow rate. For a mass flow rate of 85 kg/s a maximal efficiency of 56.13 % is reached due to the minimal temperature difference of 3 K in the LHT-preheater. Compared to R245fa/R245fa an increase in efficiency of 4.7 % can be reached by choosing R600a in both ORC units. In case of R134a/R600a and R134a/R245fa the gross second law efficiency shows a local maximum. In addition to the pinch point limitation in the LHT-preheater, the pinch point in the LT-preheater shifts from the outlet to the inlet of the heat exchanger. This leads to a minimal temperature of the geothermal fluid in state point F for a certain LHT mass flow rate (see Figure 8). As a result, the maximal gross second law efficiency for the working fluid R134a/R600a is 58.71 % for a LHT mass flow rate of 80 kg/s. For higher LHT mass flow rates, the temperature of the geothermal fluid in state point F remain constant and additionally, the temperature of the geothermal fluid in state point G increases. A lower amount of thermal energy is coupled to the double-stage ORC for LHT mass flow rates higher than 80 kg/s and consequently the second law efficiency decreases.

4.3.2 Concepts

The investigated double-stage ORC is compared to a state-of-the-art concept, a single-stage ORC with pure working fluids, and another innovative approach, a single-stage ORC with zeotropic fluid mixtures (Angelino and Colonna di Paliano, 1998 and Heberle et al., 2012). For the single-stage ORC R245fa, R134a and R600a are considered as working fluids. In addition, simulations for the single-stage ORC with the mixtures R134a/R245fa, R245fa/R365mfc and R600a/R601a are performed. The mole concentration for R134a/R245fa and R600a/R601a is 90 % of the more volatile component (R134a and R600a). In case of R245fa/R365mfc an equimolar composition is chosen. The selected mixtures show zeotropic characteristics, so that at evaporation and condensation a temperature glide can be observed. This leads to a better match of the temperature profiles of heat source or sink and ORC compared to pure fluids. For the simulations again the geothermal conditions of Kirchstockach are chosen. The

boundary conditions for the ORC are defined equally compared to the double-stage concept. This includes the pinch points of the heat exchangers, subcooling at the outlet of the air-cooled condenser, neglecting heat losses and the maximal ORC pressure ($0.8 \cdot p_{crit}$). As isentropic efficiency of the turbine for the single-stage concept 85 % is defined according to Astolfi et al. (Astolfi et al., 2014). All single-stage simulations are performed without internal recuperator and the maximum ORC process pressure is chosen according to the efficiency maximum. For the working fluids R134a and R134a/R245fa, a superheating of 10 K at the outlet of the evaporator is assumed to avoid droplets in the turbine. A comparison between the single-stage ORC with the pure fluid R245fa and the zeotropic mixture R134a/R245fa shows the temperature, enthalpy flow-diagram of Figure 9.

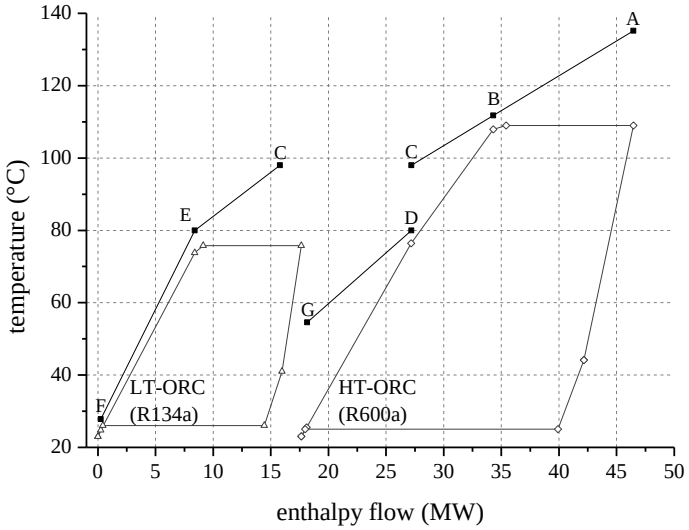

Figure 8: Temperature, enthalpy flow-diagram for a double-stage ORC using R134a (LT) and R600a (HT) as working fluids

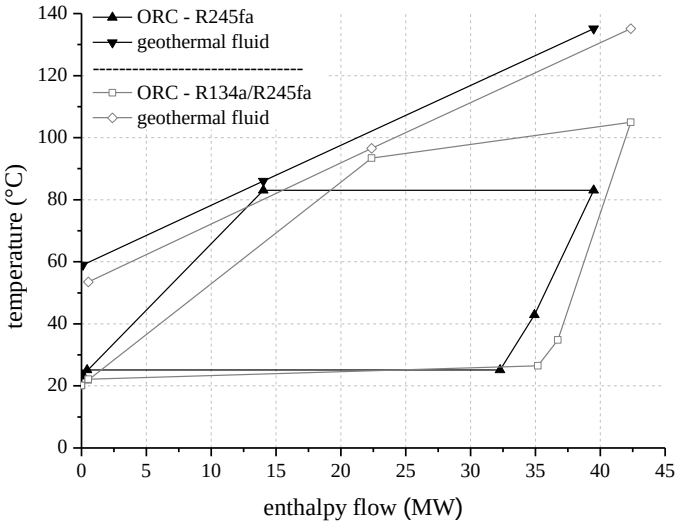

Figure 9: Temperature, enthalpy flow-diagram for single-stage ORC using R245fa and the mixture R134a/R245fa as working fluids

Due to the better match of the temperature profiles a higher amount of thermal energy is coupled to the ORC with the zeotropic mixture as working fluid. The reinjection temperature of the geothermal fluid can be decreased from 59 °C to 53.5 °C compared to the ORC with R245fa. As a result, the heat input is 2.85 MW higher and the electrical power output is 1.01 MW (22.58 %) higher. An overview of the gross and net second law efficiency of considered power plant concepts is shown in Figure 10. In addition, a double-stage concept without splitting the geothermal mass flow is included in the analysis (R245fa 2st).

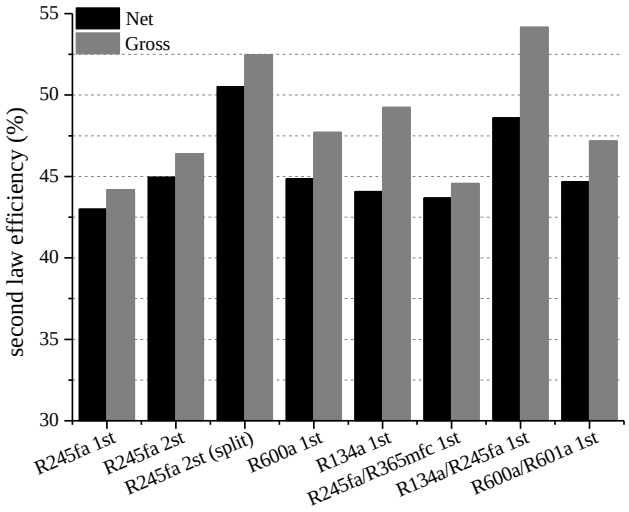

Figure 10: Net and gross second law efficiency of the selected concepts at same geothermal boundary conditions

The single-stage concept (1st) with the mixture R134a/R245fa as working fluid leads with 54.17 % to the highest gross second law efficiency. However, as well as the single-stage ORC with R600a or R134a, the power of the feed pump is relatively high. Due to the low power requirements of the feed pumps, the double-stage concept (R245fa 2st (split)) realized in Kirchstockach leads with 50.52 % to the most efficient technical solution regarding the net second law efficiency. In the simulations, the reinjection temperature of the geothermal fluid is limited to 50 °C due to the rising risk of mineral deposits in the heat exchanger for lower temperatures. The described limitation has a significant influence regarding the ORC with R134a. If lower reinjection temperatures would be possible the pinch point shifts to the inlet of the preheater and a gross second law efficiency of 60.83 % (net second law efficiency 54.46%) is obtained. The reinjection temperature in this case is 29.8 °C. In this context, another advantage of fluid mixtures as working fluids next to the temperature glide at phase change becomes apparent; by adding higher boiling component like R245fa to R134a, the fluid properties can be adapted to the boundary conditions. As a result, an efficient cycle and a reinjection temperature above 50 °C are realizable. To sum up: Optimization strategies like the selection of an appropriate pure fluid or a double-stage concept without mass flow split lead to an increase in net efficiency in the range of 1.61 % and 4.59 % compared to the single-stage ORC with R245fa. For the given geothermal boundary conditions, only the double-stage concept with geothermal mass flow split and the single-stage with R134a/R245fa lead to a significant efficiency increase (17.50 % and 13.05 %)

3. CONCLUSIONS

The comparisons of real power plant data and process simulations for the examined double-stage ORC in Kirchstockach (Germany) match very well. However, significant deviations for the calculation of the enthalpy difference at expansion between RefProp and StanMix should be highlighted. Especially for saturated or slightly superheated states at turbine inlet, as they are common for ORC, these differences have to be taken into account. Analyses of the fluid properties show that differences mainly for the liquid heat capacity. Responsible for the deviations of the behavior in the *T*,*s*-diagram are the considered heat capacity of the ideal gas and differences in the structure of the EOS. A validation or clear statement concerning the reliability of the examined EOS is not possible due to the lack of experimental data in the gas phase.

Regarding the optimization potential of the investigated double-stage concept a variation of geothermal LHT mass flow rate shows that maximum second law efficiency is reached at 80 kg/s due to the pinch point limitations in the LHT preheater. Regarding alternative power plant concepts the use of the zeotropic mixture R134a/R245fa in a single-stage ORC leads to a higher gross second law efficiency compared to the examined double-stage concept. However, systems using low-boiling working fluids like R134a and R600a show high power requirements for the feed pumps. In this context the double-stage ORC with R245fa leads to the highest net second law efficiency.

Next to the described thermodynamic aspects, economic and legal requirements concerning safety issues or feed-in tariffs have a significant influence on the choice of the power plant concept. In further work such aspects will be integrated into the analysis in form of case studies. In addition, potential concepts for combined heat and power generation will be examined for the double-stage concept in form of quasi steady-state and dynamic simulations.

REFERENCES

Aneke, M., Agnew, B., Underwood, C.: Performance analysis of the Chena binary geothermal power plant, *Applied Thermal Engineering*. **31**, (2011), 1825–1832.

Angelino, G., Colonna di Paliano, P.: Multicomponent Working Fluids for Organic Rankine Cycles (ORCs), *Energy* **23**, (1998), 449–463.

Astolfi, M., Romano, M.C., Bombarda, P., Macchi, E.: Binary ORC (organic Rankine cycles) power plants for the exploitation of medium–low temperature geothermal sources – Part A: Thermodynamic optimization, *Energy* **66**, (2014), 423–434.

Bayerisches Landesamt für Umweltschutz: Niedertemperaturverstromung mittels ORC-Anlage im Werk Lengfurt der Heidelberger Zement AG, (2001), (in German).

Bertani, R.: What is geothermal potential? *Newsletter of the International Geothermal Association* **53**, (2003), 1–3.

DiPippo, R.: Small geothermal power plants: design, performance and economics, *GHC Bulletin* (1999), 1–8.

DiPippo, R.: Geothermal Power Plants. Elsevier Science, Oxford, (2005).

Drescher, U.: Optimierungspotential des Organic Rankine Cycle für biomassebefeuerte und geothermische Wärmequellen (*Dissertation*), Bayreuth, (2008) , (in German).

Heberle, F., Preißinger, M., Brüggemann, D.: Zeotropic mixtures as working fluids in Organic Rankine Cycles for low-enthalpy geothermal resources, *Renewable Energy* **37** , (2012), 364-370.

Hwang, S., DesMarteau, D.D., Beyerlein, A.L., Smith, N.D., Joyner, P.: The heat capacity of fluorinated propane and butane derivatives by differential scanning calorimetry, *Journal of Thermal Analysis*, **38**, (1992), 2515–2538.

Kanoglu, M.: Exergy analysis of a dual-level binary geothermal power plant, *Geothermics* **31**, (2002), 709–724.

Kosmadakis, G., Manolakos, D., Kyritsis, S., Papadakis, G.: Design of a two stage Organic Rankine Cycle system for reverse osmosis desalination supplied from a steady thermal source, *Desalination* **250**, (2010a) 323–328.

Kosmadakis, G., Manolakos, D., Papadakis, G.: Parametric theoretical study of a two-stage solar organic Rankine cycle for RO desalination, *Renewable Energy* **35**, (2010b), 989–996.

Kunz, O., Klimeck, R., Wagner, W., Jaeschke, M.: The GERG-2004 Wide-Range Equation of State for Natural Gases and Other Mixtures - GERG Technical Monograph, 15, *VDI-Fortschritts-Bericht*, Düsseldorf (2007).

Lemmon, E.W., Span, R.: Short fundamental equations of state for 20 industrial fluids, *Journal of Chemical Engineering Data* **51**, (2006), 785–850.

Lemmon, E.W., Huber, M.L., McLinden, M.O.: NIST Standard Reference Database 23 – Version 9.1. Physical and Chemical Properties Division. National Institute of Standards and Technology, Boulder, Colorado, US Department of Commerce, USA, (2013).

Meinel, D., Wieland, C., Spliethoff, H.,. Effect and comparison of different working fluids on a two-stage organic rankine cycle (ORC) concept. *Applied Thermal Engineering* **63**, (2014), 246–253.

Peng, D.-Y., Robinson, D.B.: A New Two-Constant Equation of State. *Industrial and Engineering Chemistry Fundamentals*, **15**, (1976), 59–64.

Preißinger, M., Heberle, F., Brüggemann, D.: Thermodynamic analysis of double-stage biomass fired Organic Rankine Cycle for micro-cogeneration. *International Journal of Energy Research*, **36**, (2012), 944–952.

Smolen, S.: Simulation and thermodynamic analysis of a two-stage Organic Rankine Cycle for utilization of waste heat at medium and low temperature levels. *Energy Science and Technologies*, **1**, (2011), 64–78.

Soave, G., 1972. Equilibrium constants from a modified Redlich-Kwong equation of state. *Chemical Engineering. Science*, **27**, 1197–1203.

Stefansson, V.: Competitive status of geothermal energy, *Proceedings*, World Geothermal Congress. Beppu - Morioka, Japan, (2000).

Walraven, D., Laenen, B., D´haeseleer, W.: Comparison of thermodynamic cycles for power production from low-temperature geothermal heat sources. *Energy Conversion and Management*, **66**, (2013), 220–233.

Woudstra, N., van der Stelt, T.P.: Cycle-Tempo: a program for the thermodynamic analysis and optimization of systems for the production of electricity, heat and refrigeration. Energy Technology Section, Delft University of Technology, The Netherlands, (2002).